Plant Physiology, December 1999, Vol. 121, pp. 1117–1126, www.plantphysiol.org © 1999 American Society of Plant Physiologists

Molecular Dissection of the Role of Histidine in Nickel Hyperaccumulation in *Thlaspi goesingense* (Hálácsy)[1]

Michael W. Persans, Xiange Yan, Jean-Marc M.L. Patnoe, Ute Krämer, and David E. Salt*

Northern Arizona University, P.O. Box 5698, Flagstaff, Arizona 86011 (M.W.P., J.-M.M.L.P., D.E.S.); Rutgers University, Waksman Institute, Piscataway, New Jersey 08854 (X.Y.); and Fakultät für Biologie, W 5, Universität Bielefeld, 33615 Bielefeld, Germany (U.K.)

To understand the role of free histidine (His) in Ni hyperaccumulation in *Thlaspi goesingense*, we investigated the regulation of His biosynthesis at both the molecular and biochemical levels. Three *T. goesingense* cDNAs encoding the following His biosynthetic enzymes, ATP phosphoribosyltransferase (*THG1*, GenBank accession no. AF003347), imidazoleglycerol phosphate dehydratase (*THB1*, GenBank accession no. AF023140), and histidinol dehydrogenase (*THD1*, GenBank accession no. AF023141) were isolated by functional complementation of *Escherichia coli* His auxotrophs. Northern analysis of *THG1*, *THD1*, and *THB1* gene expression revealed that each gene is expressed in both roots and shoots, but at the concentrations and dosage times of Ni treatment used in this study, these genes failed to show any regulation by Ni. We were also unable to observe any increases in the concentration of free His in root, shoot, or xylem sap of *T. goesingense* in response to Ni exposure. X-ray absorption spectroscopy of root and shoot tissue from *T. goesingense* and the non-accumulator species *Thlaspi arvense* revealed no major differences in the coordination of Ni by His in these tissues. We therefore conclude that the Ni hyperaccumulation phenotype in *T. goesingense* is not determined by the overproduction of His in response to Ni.

There are certain plants, such as *Thlaspi goesingense*, that have the ability to accumulate concentrations of Ni in their shoots far exceeding those observed in the soil, without suffering the detrimental effects of Ni toxicity (Reeves and Brooks, 1983). Brooks et al. (1977) first used the term "hyperaccumulator" to describe plants that contain >1,000 $\mu g\ g^{-1}$ (0.1%) Ni in their dried leaves, a concentration at least an order of magnitude higher than Ni levels in nonaccumulator species. Progress is being made in understanding the mechanisms involved in metal hyperaccumulation, but the molecular basis of this intriguing phenomenon remains elusive (Salt and Krämer, 1999).

Recent work on the mechanism of Ni hyperaccumulation in *T. goesingense* has established that Ni tolerance is a primary determinant of the hyperaccumulation phenotype in hydroponically cultured plants (Krämer et al., 1997). An important component of this Ni tolerance mechanism appears to be based on the efficient intracellular compartmentalization of the Ni into the vacuole (U. Krämer and D.E. Salt, unpublished data).

Recently, Krämer et al. (1996) observed a 36-fold increase in the concentration of free His in the xylem exudate of the Ni hyperaccumulator *Alyssum lesbiacum* after exposure to Ni. However, no significant change was observed in the nonaccumulator *Alyssum montanum*. The authors also observed a significant linear correlation in the xylem exudate concentrations of free His and Ni in several Ni hyperaccumulators in the genus *Alyssum* (Krämer et al., 1996). Because His is an effective chelator of Ni at cytoplasmic pH (Dawson et al., 1986), the authors suggested that His may be involved in chelating Ni during the transport and or storage of Ni in the *Alyssum* Ni hyperaccumulators. This was supported by the use of x-ray absorption spectroscopy, which identified putative Ni-His complexes in the xylem sap, root, and shoot tissue of *A. lesbiacum* (Krämer et al., 1996). However, the mechanism by which Ni hyperaccumulation is achieved through the action of His has not been established.

Both *Alyssum* and *Thlaspi* Ni hyperaccumulator species are members of the Brassicaceae family, suggesting that free His may also play a role in the mechanism of Ni hyperaccumulation in *T. goesingense*. This is supported by the recent identification of putative Zn-His complexes in the roots of the closely related Zn hyperaccumulator *Thlaspi caerulescens* (Salt at al., 1999b). Therefore, to determine if free His is involved in Ni hyperaccumulation in *T. goesingense*, we investigated the regulation of His biosynthesis at both the molecular and biochemical levels in *T. goesingense*.

To determine if Ni regulates the expression of genes involved in His biosynthesis in *T. goesingense*, we cloned genes encoding ATP phosphoribosyltransferase (*THG1*), imidazoleglycerol phosphate dehydratase (*THB1*), and histidinol dehydrogenase (*THD1*), enzymes that catalyze potentially rate-limiting steps in His biosynthesis.

Previously, several authors have published the sequences of various His biosynthetic genes, including *HisD* (encoding histidinol dehydrogenase [HDH]) from Arabidopsis (Bevan et al., 1998) and *Brassica oleracea* (Nagai et al., 1991); *HisB* (encoding imidazoleglycerol phosphate dehydratase [IGPD]) from *Pisum sativum* (Kim and Theologis, 1996), *Triticum aestivum*, and Arabidopsis (Tada et al.,

[1] This research was supported by grants from the U.S. Department of Energy, Environmental Management Science program (no. DE–FG07–98ER20295 to D.E.S.) and a North Atlantic Treaty Organization fellowship awarded to U.K. by the German Academic Exchange Service (DAAD).

* Corresponding author; e-mail david.salt@nau.edu; fax 520–523–8111.

1994); *HisC* (encoding L-histidinol phosphate aminotransferase [HPA]) from *Nicotiana tabacum* (El Malki et al., 1998); and *HisIE* (encoding phosphoribosyl-ATP pyrophosphohydrolase/phosphoribosyl-AMP cyclohydrolase [PR-ATP/PR-AMP]) from Arabidopsis (Fujimori and Ohta, 1998). However, to our knowledge, this is the first study to isolate ATP phosphoribosyltransferase (ATP-PRT), the enzyme that catalyzes the first committed step in His biosynthesis, from plants.

To examine the effects of Ni exposure on His biosynthesis, we also measured the concentration of free His in the roots, shoots, and xylem sap in both the Ni hyperaccumulator *T. goesingense* and the nonaccumulator *Thlaspi arvense*. Additionally, we quantified putative Ni-His complexes in both *T. goesingense* and *T. arvense* using x-ray absorption spectroscopy.

MATERIALS AND METHODS

Plant Growth Conditions and Ni Treatment

For cDNA library construction, *Thlaspi goesingense* seeds were germinated and grown hydroponically according to the method of Krämer et al. (1997). The plants were exposed to 25 μM $Ni(NO_3)_2$ for 5 weeks with two exchanges of hydroponic solution per week. After 5 weeks, whole plants were harvested, immediately frozen in liquid nitrogen, and stored at −80°C.

Plants for RNA and genomic DNA studies were grown as follows. Seeds were germinated on filter papers moistened with double-distilled water for 7 d and subsequently transferred to hydroponic culture solution according to the method of Krämer et al. (1997). Plants were maintained on a 12-h d period and day/night temperature of 25°C/20°C, with weekly changes of hydroponic culture solution. Both fluorescent and incandescent lights were used to provide 170 μmol m^{-2} s^{-1} of photosynthetic photon flux (PPF) at the level of the plants. After 6 weeks of growth from the date of transfer into the hydroponic culture solution, plants were exposed to 50 μM Ni for 24 or 48 h by the addition of $Ni(NO_3)_2$ to the culture solution. Both roots and shoots were harvested separately, immediately frozen in liquid nitrogen, and stored at −80°C. For the efficient isolation of RNA from shoot material, it was necessary to deplete the plants of starch. This was achieved by harvesting treated plants just before the onset of the light period.

His Levels in *T. goesingense*

For analysis of the free His concentration, root and shoot material was extracted as follows. Approximately 2 g of tissue was frozen in liquid nitrogen and ground to a fine powder in a pestle and mortar. To the frozen powder 6 mL of 3% (w/v) sulfosalicylic acid was added and the slurry ground until the plant tissue had completely thawed. The slurry was then centrifuged at 1,550*g* for 15 min at room temperature. The supernatant was filtered through a 0.45-μm filter to remove suspended particulate material. Phenylthiocarbamyl derivatization was carried out following the method of Fierabracci et al. (1991). The nonbiological amino acid Met sulfoxide was added to 10 μL of tissue extract or xylem exudate to a final concentration of 40 μM and used during analysis as an internal standard. Samples were vacuum-dried (model SVC200, Savant Instruments, Holbrook, NY), redissolved in 20 μL of ethanol:water:TEA (2:2:1, v/v), and vacuum-dried again. To the dried samples 20 μL of ethanol:triethylamine (TEA):water:phenyl isothiocyanate (7:1:1:1, v/v) was added, and the samples incubated at room temperature for 20 min. Samples were vacuum-dried to remove excess reagent and reconstituted in 250 μL of phosphate buffer (pH 7.4). Separation of the phenylthiocarbamyl amino acid derivatives was performed on a Nucleosil C_{18} 5-μm HPLC column (Sigma, St Louis) (250 × 4.6 mm) at 38°C. The elution solvent consisted of 0.14 M sodium acetate in water plus 0.5 mL/L TEA, titrated to pH 6.4 with glacial acetic acid, with the addition of 60 mL/L acetonitrile (solvent A); and 60% (v/v) acetonitrile in water (solvent B). Phenylthiocarbamyl amino acid derivatives were detected at 254 nm using an UV spectrophotometer (Spectroflow 783, Kratos Analytical, Ramsey, NJ).

Determination of Ni Speciation in *Thlaspi*

Plant samples were shipped to the Stanford Synchrotron Radiation Laboratory (Stanford University, Stanford, CA) on dry ice. To minimize breakdown and mixing of cellular components within the plant material, care was taken to keep the tissue frozen at all times prior to measurement. To this end, frozen plant tissues were carefully ground under liquid nitrogen and compacted into liquid-nitrogen-cooled 1-mm pathlength lucite sample holders with mylar windows. Aqueous model compounds were diluted by 30% to 50% (v/v) with glycerol (to avoid ice crystal formation) before being pipetted into holders and rapidly frozen in liquid nitrogen. During data collection, samples were held at approximately 15 K using a flowing liquid helium cryostat.

X-ray absorption spectroscopy was carried out on beamline 7–3 of the Stanford Synchrotron Radiation Laboratory using a Si(220) double crystal monochromator, 1-mm upstream vertical aperture, and no focusing optics. Incident intensity was measured using a nitrogen-filled ion chamber, and the absorption spectrum was collected in fluorescence using a 13-element germanium detector (Cramer et al., 1988) by monitoring the Ni $K_{\alpha a}$ fluorescence line at 7,472 eV. Spectra were energy calibrated with respect to a spectrum of Ni foil, and collected simultaneously with the spectrum of each sample, the first energy inflection of which was assumed to be 8,333 eV.

X-ray absorption spectroscopy data reduction was carried out using the EXAFSPAK suite of programs (George, 1998) according to standard methods (Koningsberger and Prins, 1988). Quantitative edge-fitting analysis was performed using the program DATFIT (George et al., 1991). Here, the near-edge spectrum of the plant material is fit using a least-squares algorithm to a linear combination of edge spectra from a library of Ni model compounds. The fractional contribution of each model spectrum to the fit is then directly proportional to the percentage of Ni present in that form in the plant material. By analyzing the total Ni

content of the tissue samples, the percentage fractional contribution can then be simply converted into the absolute amount of complex present.

Total RNA Isolation and λTriplEx cDNA Library Construction

Total RNA was isolated according to the method of Murphy and Taiz (1995) as follows. Frozen Ni-treated plant material (3–4 g) was ground in liquid nitrogen to a fine powder using a pre-chilled mortar and pestle. The ground tissue was added to 3.5 mL of extraction buffer (1% [w/v] triisopropylnapthylenesulfonic acid, 6% [w/v] *p*-aminosalicylic acid, 1% [w/v] NaCl, 3% [w/v] polyvinylpyrrolidine, 5% [v/v] β-mercaptoethanol, 4 M guanidine thiocyanate, and 25 mM sodium citrate), shaken gently to mix, and incubated for 5 min at room temperature after the tissue had thawed. To the samples, 3.5 mL of dilution buffer (6× SSC, 10 mM Tris, 1 mM EDTA, and 0.25% [w/v] SDS) was added and vortexed for 1 min, then incubated at 65°C for 5 min.

Phenol (6 mL) was added and the mixture was vortexed for 1 min and incubated at room temperature for 5 min. Chloroform (6 mL) was added and the mixture was vortexed for 1 min. Samples were then centrifuged at 5,000*g* for 10 min at 4°C to separate the phases. The upper aqueous phase was removed, 7 mL of phenol and 10 mL of chloroform were added, and the mixture was vortexed for 1 min, incubated at room temperature for 5 min, and vortexed again for 1 min. The phases were then separated by centrifugation at 3,000*g* for 10 min at 4°C. The upper aqueous layer was removed and 7 mL of isopropanol was added and the sample incubated for 4 h at −20°C to precipitate the RNA. RNA was collected by centrifugation at 13,500*g* for 15 min, and the pellet was resuspended in 400 μL of diethyl pyrocarbonate (DEPC)-treated water. The resuspended pellet was then re-extracted in 1 mL of 5 M LiCl by vortexing for 1 min, and RNA was reprecipitated by incubation at −20°C for 45 min. The RNA was pelleted by centrifugation at 27,000*g* for 25 min at 4°C. The RNA pellet was washed by the addition of 1 mL of 70% (v/v) ethanol and collected by centrifugation at 27,000*g* for 25 min at 4°C. The final purified RNA was resuspended in 100 μL of DEPC-treated water and stored at −80°C.

The total *T. goesingense* RNA was sent to CLONTECH Laboratories (Palo Alto, CA), where mRNA isolation, cDNA synthesis, and construction of recombinant λTriplex were performed. The cDNA synthesis resulted in 1.6×10^6 independent clones with an average insert size of 2.0 kb (range 0.7–4.0 kb). All *T. goesingense* cDNAs were cloned into the *Eco*RI and *Xho*I sites within the λTriplEx multiple cloning site and converted to the phagmid pTriplEx using a cre-recombinase *Escherichia coli* expressing strain (BM25.8).

The choice of the λTriplEx vector was made because of several of its unique features. Each vector has separate initiation codons in two differing frames, both followed by a single poly-dT tract (slip site) that allows either the RNA polymerase or the ribosomes to skip nucleotides, thereby allowing reading in all three frames. Furthermore, the vector incorporates the 5′-untranslated region (UTR) of the *omp*A gene from *E. coli* to increase mRNA stability. These features allow every recombinant vector to express some protein, regardless of the initial frame of the insert.

Cell Transformation and Functional Complementation in *E. coli*

T. goesingense cDNAs encoding functional homologs of the *E. coli* His biosynthetic enzymes ATP-PRT, IGPD, and HDH were isolated by screening for cDNAs that could complement the His requirement of various His auxotrophic *E. coli* mutants. *E. coli* lacking a functional copy of the gene encoding ATP-PRT (strain KL738), IGPD (strain SB3930), or HDH (strain UTH4758) were transformed with the *T. goesingense* pTriplEx cDNA library by electroporation (model EC100 Electroporator, EC Apparatus, St. Petersburg, FL), per the manufacturer's protocol. Transformed cells were selected on Luria-Bertani medium and ampicillin (100 μg mL^{-1}) agar plates, resulting in 10^6 to 10^7 transformants/μg pTriplEx plasmid DNA. The resulting colonies were replica plated onto M-9 minimal media supplemented with 19 amino acids (excluding His), each at a concentration of 25 μg mL^{-1}, 0.1 mM isopropylthiogalactoside, and ampicillin (100 μg mL^{-1}). Colonies that were able to grow were retested for growth on M-9 minimal medium lacking His. Plasmid DNA was isolated from colonies that grew after replating, and the ability of these plasmids to complement the His requirement of the *E. coli* auxotrophic mutants was confirmed by retransformation of the appropriate His auxotrophic *E. coli* mutant.

Sequencing and Analysis

Double-stranded DNA from all three genes was completely sequenced using pTriplEx plasmid primers and primers based on previous sequence data using a DNA sequencer (model 373, Applied Biosystems, Foster City, CA) and a dye terminator cycle sequencing ready reaction kit (catalog no. P/N 402078, ABI PRISM, Perkin-Elmer, Foster City, CA).

Predicted translations of the *THG1*, *THD1*, and *THB1* genes were generated and a search was performed to identify any homologous sequences in GenBank. The *THG1* predicted amino acid sequence was aligned with existing ATP-PRT sequences acquired from GenBank using the CLUSTAL_W algorithm (Thompson et al., 1994). The predicted amino acid sequence of *THB1* and *THD1* was aligned with existing plant sequences using ALIGN (Myers and Miller, 1989). A phylogenetic construction of the resulting aligned sequences for THG1 (ATP-PRT) was also performed using the PHYLIP algorithm (Phylogeny Inference Package, version 3.57c, Department of Genetics, University of Washington, Seattle) (Felsenstein, 1993). Both the alignment and phylogenetic analysis was performed at the University of Illinois Biology Workbench (http://biology.ncsa.uiuc.edu/). Analysis for the presence and type of protein targeting sequence was performed using the PSORT algorithm (Nakai and Kanehisa, 1992) found at http://psort.nibb.ac.jp:8800/. The targeting sequence cleav-

age site was predicted using the SignalP (version 1.1) algorithm (Nielsen et al., 1997) found at http://www.cbs.dtu.dk/services/SignalP/.

Nucleotide Probe Preparation

One-hour restriction digests of pTriplEx-(*THG1*) and pTriplEx-(*THD1*) with *Xho*I, pTriplEx-(*THB1*) with *Eco*RI and *Xho*I, and an Arabidopsis actin gene (GenBank accession no. U37281) with *Bam*HI and *Eco*RI were performed at 37°C. The resulting fragments were run on a 1.5% (w/v) agarose gel and the appropriate size fragment was excised for the gel and recovered by electroelution. For *THG1* and *THD1*, the resulting fragments were approximately 400 and 500 bp in size, respectively, and both contained the 3′-UTR of the gene. For *THB1*, the entire cDNA was recovered. The resulting actin probe was approximately 950 bp and did not contain either 5′- or 3′-UTRs, only the protein coding sequence.

In advance of blot hybridization, 75 to 150 ng of DNA (approximately 5 μL) was denatured at 100°C for 10 min in 35 μL of double-distilled water, and the sample was snap-cooled on ice for 30 s. Then, 2 μL of bovine serum albumin (BSA) (10 mg/mL), 10 μL of 5× OLB buffer (250 mM Tris-HCl [pH 8.0], 25 mM $MgCl_2$, 0.35% [v/v] β-mercaptoethanol, 100 μM each dGTP, dCTP, and dTTP, 1 M HEPES [pH 6.0], and 0.54 μg/μL pdN_6 random hexamers), 2 to 3 μL of [α-^{32}P]dATP (10 μCi/μL), and 5 units of DNA polymerase I Klenow fragment was added to the denatured DNA. The labeling reaction was incubated for at least 5 h at room temperature. The labeled DNA probe was boiled for 10 min, snap-cooled on ice for 30 s, centrifuged for 10 s at 14,000*g*, and added directly to the hybridization buffer.

Southern Analysis

To obtain genomic DNA, 0.5 to 1.0 g of frozen *T. goesingense* shoot tissue was placed in a 15-mL centrifuge tube (Falcon 2059, Becton Dickinson, Lincoln Park, NJ), frozen in liquid nitrogen, and ground to a fine powder with a glass rod. Urea extraction buffer (700 μL; 7 M urea, 312 mM NaCl, 20 mM EDTA, 1% [w/v] *N*-lauroyl sarkosine, and 50 mM Tris-HCl [pH 8.0]) was added, and the sample was thawed to room temperature with frequent gentle mixing. Phenol/chloroform (1:1, 500 μL) was added and the sample was incubated for 15 min at 37°C in a rotary shaker. The sample was then transferred to a 1.5-mL microfuge tube and the aqueous phase was separated by centrifugation at 14,000*g* for 10 min. The upper aqueous phase (approximately 500 μL) was removed and placed in a fresh 1.5-mL microfuge tube. To the aqueous phase 50 μL of 4.4 M ammonium acetate and 700 μL of isopropanol were added, the sample was mixed well, and the genomic DNA pelleted by centrifugation at 14,000*g* for 1 min. The genomic DNA pellet was resuspended in 500 μL of sterile water and reprecipitated as above. The final DNA pellet was washed once with 70% (v/v) ethanol, spun at 14,000*g* for 3 min, air-dried for 10 to 15 min inverted on a paper towel, and resuspended in 50 to 100 μL of sterile water.

For genomic Southern analysis, genomic DNA was digested with 60 units of each of the following restriction enzymes: *Bam*HI, *Eco*RI, *Hin*dIII, *Xba*I, *Xho*I, or *Pst*I, for 6 to 8 h at 37°C. The resulting fragments were electrophoresed in a 0.8% (w/v) agarose Tris-boric acid-EDTA gel, and capillary blotted onto nylon membranes (catalog no. 80–6221–93, Pharmacia Biotech, Piscataway, NJ) overnight using 10× SSC. The genomic DNA was UV-crosslinked (model FB–UVXL–1000, Fisher Scientific, Loughborough, Leicestershire, UK) to the membrane. The blots were prehybridized at 65°C for at least 2 h in 10 mL of a prehybridization solution containing 50 mM Tris-HCl (pH 8.0), 10 mM EDTA (pH 8.0), 5× SSC, 5× Denhardt's solution, 0.2% (w/v) SDS, 7.5% (w/v) dextran sulfate, and 100 μg mL^{-1} sheared salmon-sperm DNA. The blots were then probed with a denatured ^{32}P-labeled probe added directly to the hybridization solution and the blots incubated at 65°C for 12 to 16 h. After hybridization the blots were rinsed with 50 mL of 2× SSC and 0.1% (w/v) SDS for 5 min at room temperature and then washed two to four times for 15 min at 65°C with 50 mL of 0.1× SSC and 0.1% (w/v) SDS. After washing, the membranes were placed on x-ray film and exposed at −80°C for 10 to 16 h.

Northern Analysis

Total RNA was isolated according to the method of Puissant and Houdebine (1990). Approximately 5 to 10 g of 6-week-old *T. goesingense* shoots or roots were frozen in liquid nitrogen and ground to a fine powder in a chilled mortar and pestle. The ground tissue was placed in four to six centrifuge tubes each containing 5 mL of GuISCN extraction buffer (4 M guanidinium isothycyanate, 25 mM sodium citrate [pH 7.0], 0.5% [w/v] *N*-lauroyl sarkosine, and 0.1 M β-mercaptoethanol), and the tubes were mixed by inversion.

The samples were mixed with 0.1 volume of 2 M sodium acetate (pH 4.0) and 5 mL of phenol:chloroform (5:1) was added. The samples were mixed and centrifuged at 5,000*g* for 15 min at 4°C. The aqueous phase (approximately 7 mL) was removed and placed in a fresh 15-mL centrifuge tube, and RNA was precipitated by adding an equal volume of isopropanol at 4°C. The RNA was collected by centrifugation at 4,000*g* for 10 min at 4°C, and each pellet was resuspended in 2 mL of 4 M LiCl, mixed well, and recentrifuged at 4,000*g* for 10 min at 4°C. Each pellet was resuspended in 2 mL of Tris-EDTA buffer containing 0.5% (w/v) SDS, and an equal volume of chloroform was added. After mixing and centrifugation at 4,000*g* for 10 min at 4°C, the upper aqueous phase was removed and the total RNA precipitated after adding 0.1 volume of 2 M sodium acetate (pH 5.0) and an equal volume of isopropanol. The total RNA was collected by centrifugation at 4,000*g* for 15 min at 4°C and washed with 70% (v/v) ethanol and 100% ethanol. The samples were air-dried for 15 min, resuspended in 300 μL of sterile, DEPC-treated water, and stored at −80°C.

For northern analysis, 30 μg of total RNA was electrophoresed on 1.2% (w/v) agarose-formaldehyde gels and capillary blotted overnight onto nylon membranes (catalog no. 80–6221–93, Pharmacia Biotech) using 10× SSC. The

RNA was UV-crosslinked to the membrane and the blot prehybridized in 10 mL of a pre-hybridization solution containing 200 mM Na_2PO_4 (pH 7.2), 5% (w/v) SDS, 1 mM EDTA, 10 mg/mL BSA, and 0.1 mg/mL sheared salmon-sperm DNA for at least 2 h at 65°C. The blots were probed with denatured α-^{32}P-labeled probes added directly to the hybridization solution and incubated at 65°C for 12 to 16 h. The blots were washed twice for 15 to 20 min at 65°C with 50 mL of a solution containing 40 mM Na_2PO_4 (pH 7.2), 5% (w/v) SDS, 1 mM EDTA, and 5 mg/mL BSA. The blots were then washed for a second time in 50 mL of a solution containing 40 mM Na_2PO_4 (pH 7.2), 1% (w/v) SDS, and 1 mM EDTA for 30 to 35 min at 60°C to 65°C. After washing, blots were placed on x-ray film for 1 to 4 d at −80°C.

RESULTS

Functional Complementation of *E. coli* His Mutants

T. goesingense cDNAs that encode ATP-PRT, IGPD, and HDH were isolated. These genes were designated *THG1*, *THB1* (Persans et al., 1998), and *THD1* (Persans et al., 1998), and their sequences were submitted to GenBank. When expressed in *E. coli HisG, HisB,* and *HisD* mutant strains, these cDNAs were able to complement the *E. coli* mutants' inability to grow in the absence of His (Fig. 1). This suggests that the *T. goesingense THG1*, *THB1*, and *THD1* cDNAs encode ATP-PRT, IGPD, and HDH, respectively. *THG1* is the first cDNA sequence that encodes ATP-PRT to be isolated from plants.

The predicted amino acid sequences derived from the cDNA all had high identity to several protein sequences in GenBank. The THG1 amino acid sequence had 83% identity with a putative Arabidopsis ATP-PRT expressed sequence tag (EST) (GenBank accession no. Z31670) amino acid sequence. Also, the *THG1* amino acid sequence had 29% and 26% identity to the ATP-PRT from *E. coli* (HisG) (GenBank accession no. X13462) and *Saccharomyces cerevisiae* (His1) (GenBank accession no. V01306) amino acid sequences, respectively (Fig. 2A). The THB1 amino acid sequence had 86%, 87%, and 84% identity to an Arabidopsis IGPD (GenBank accession no. 2244848), a *Triticum aestivum* IGPD (GenBank accession no. 551331), and a *Pisum sativum* IGPD (GenBank accession no. 2495230) amino acid sequence, respectively. (Fig. 2B). The THD1 amino acid sequence had 89% and 86% identity with *Brassica oleracea* HDH (GenBank accession no. 60466) (Fig. 2C) and a putative Arabidopsis EST HDH (GenBank accession no. T42850) sequence.

An analysis of the protein leader sequences for all three *T. goesingense* His biosynthetic genes predicts that both THG1 and THD1 proteins are targeted to the chloroplast, and the THB1 protein appears to be targeted to the mitochondria (Table I).

A phylogenetic tree was constructed to determine the evolutionary placement of the THG1 protein sequence in relation to existing protein sequences (Fig. 3). The THG1 amino acid sequence was closely grouped with an Arabidopsis EST encoding a putative ATP-PRT. The THG1 amino acid sequence is more distantly related to nine archaebacteria, eubacteria, and unicellular eukaryotic ATP-PRT sequences, and falls within its own unique group.

Southern Blot of *THG1*

To examine the number of *THG1* genes present in the *T. goesingense* genome, genomic DNA was digested with various restriction enzymes, run on an agarose gel, and Southern blotted. The genomic DNA was probed with an internal 400-bp *Xho*I fragment containing the 3′-UTR of the *THG1* cDNA (Fig. 4.) Of the restriction enzymes used, *Bam*HI, *Eco*RI, *Hin*dIII, *Pst*I, and *Xba*I do not cut within the *THG1* cDNA sequence and *Xho*I cuts once. As expected, *Bam*HI, *Pst*I, and *Hin*dIII digestion resulted in a single band, while digestion with *Xho*I resulted in two bands. Interestingly, *Eco*RI and *Xba*I digestion produced two

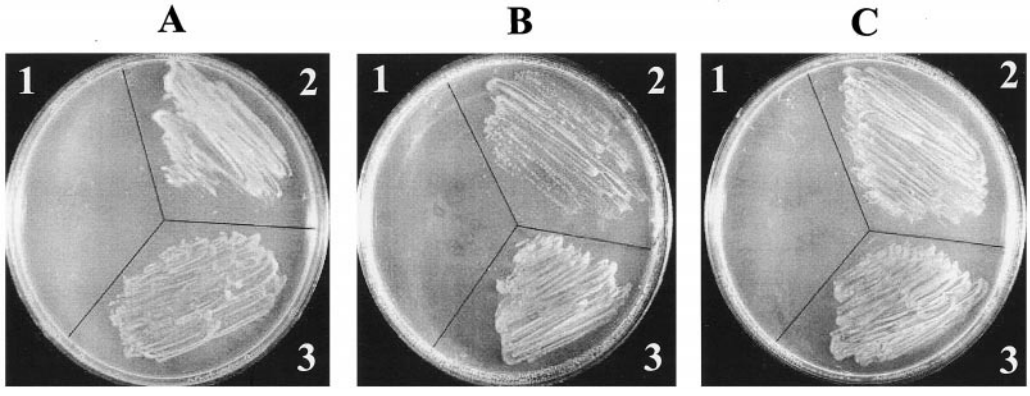

Figure 1. Functional complementation of *HisG*$^-$, *HisB*$^-$, and *HisD*$^-$ His auxotropic *E. coli* mutants with *T. goesingense* cDNAs. Three *T. goesingense* cDNAs were isolated by screening a pTriplEx cDNA library for complementation of *HisG*$^-$ (A), *HisB*$^-$ (B), and *HisD*$^-$ (C) mutations in *E. coli*. The three clones represent ATP phosphoribosyltransferase (*THG1*, accession no. AF003347), imidazolglycerol phosphate dehydratase (*THB1*, accession no. AF023140), and histidinol dehydrogenase (*THD1*, accession no. AF023141). Each plate contained the following: a mutant unable to grow in the absence of His (1); a mutant transformed with complementing *T. goesingense* cDNA (2); and a wild-type TOPP10F′ *E. coli* strain (3).

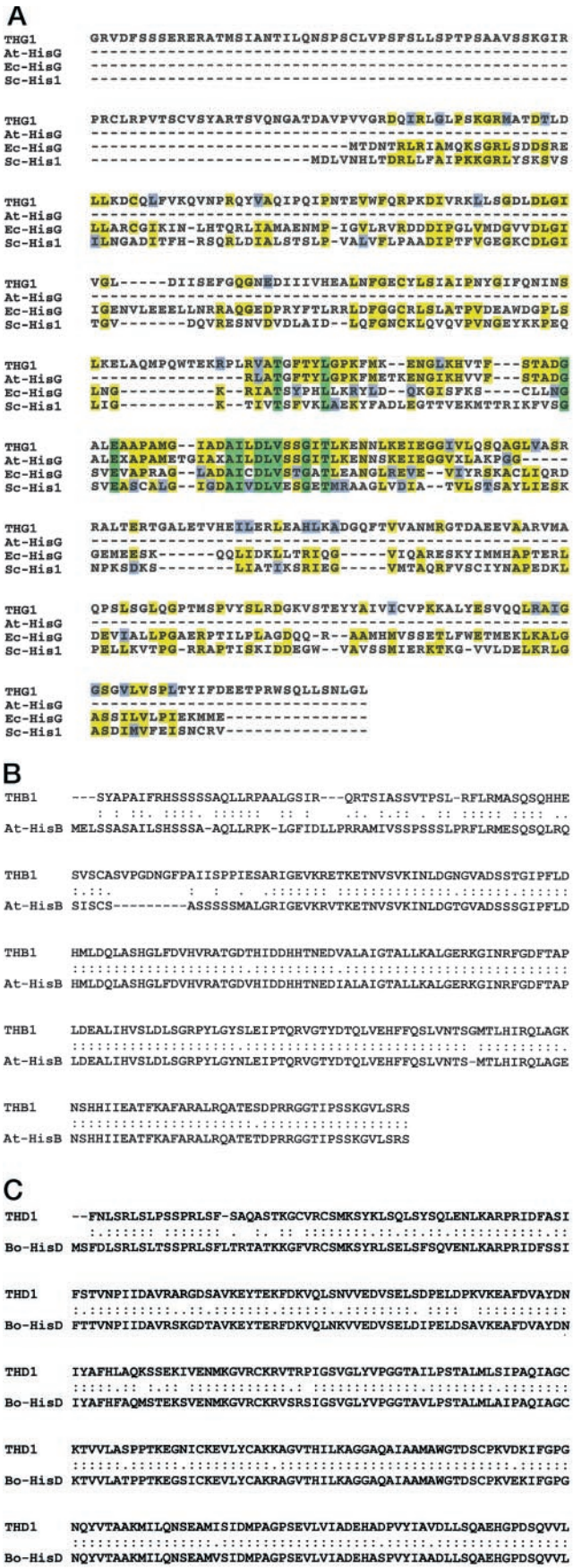

Figure 2. Alignment of the predicted amino acid sequences of *THG1*, *THB1*, and *THD1*. Sequences used are as follows. A, *T. goesingense* ATP-PRT (THG1; accession no. AF003347), Arabidopsis EST sequence (At-HisG; accession no. Z31670), *E. coli* ATP-PRT (Ec-HisG; accession no. X13462), *S. cerevisiae* ATP-PRT (Sc-His1; accession no. V01306). Green, Amino acids conserved in all aligned sequences; yellow, amino acids conserved in at least two of the aligned sequences; blue, conservative amino acid substitutions. B, *T. goesingense* (THB1; accession no. AF023140), and Arabidopsis IGPD (At-HisB; accession no. U02689). C, *T. goesingense* (THD1; accession no. AF023141), and *B. oleracea* HDH (Bo-HisD; accession no. M60466). Colons, Identity; periods, conservative replacements.

bands. This is inconsistent with the restriction map of the cloned *THG1* cDNA. This result implies that there may be more than one *THG1* gene present in the genome. However, these results are consistent with the assumption that two or perhaps a small family of *THG1* genes is present in the genome.

Ni Regulation of *THG1*, *THD1*, and *THB1* Gene Expression

Northern analysis of total RNA isolated from *T. goesingense* exposed to 50 μM Ni for 0, 24, and 48 h showed that mRNA levels of *THG1*, *THB1*, or *THD1* in both the roots and shoots are not affected by exposure to Ni in the hydroponic culture solution (Fig. 5).

Free His Concentrations and Ni Speciation

Free His concentrations in both shoots and xylem sap of the Ni hyperaccumulator *T. goesingense* did not differ significantly from those observed in the nonaccumulator *Thlaspi arvense* (Table II). However, His concentrations in the roots of *T. goesingense* were significantly higher than those observed in *T. arvense*. Interestingly, after exposure to 50 μM Ni for 7 d, His concentrations in both the shoot and xylem exudate of *T. goesingense* remained unchanged. However, His concentrations in the roots dropped to levels observed in unexposed *T. arvense* (Table II). Acid hydroly-

Table I. *Predicted target sequence of the cloned T. goesingense His biosynthetic genes*

Gene Identification (Enzyme ID)	Predicted Target Sequence Type	PSORT Score (Most Likely Candidate)	GenBank Accession No.
THG1 (ATP-PRT)	Chloroplast	5.23	AF003347
THB1 (IGPD)	Mitochondria	2.41	AF023140
THD1 (HDH)	Chloroplast	3.04	AF023141

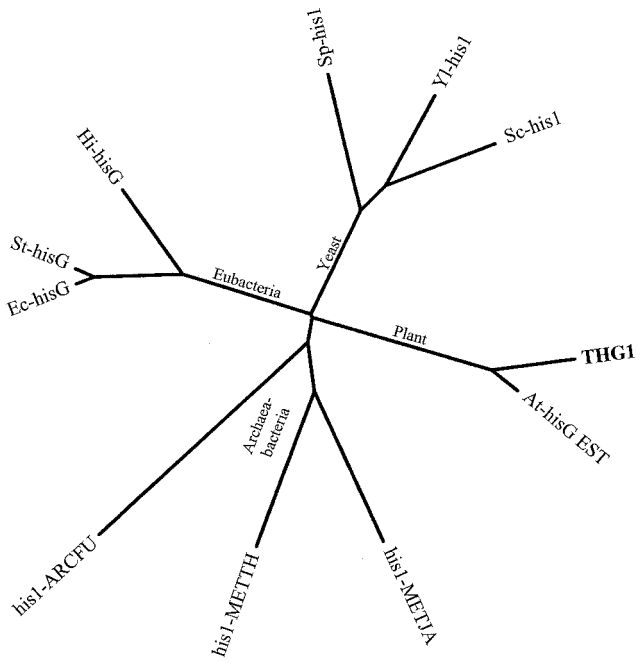

Figure 3. Unrooted phylogenetic tree of *T. goesingense* ATP-PRT and nine other ATP-PRT sequences. *T. goesingense* ATP-PRT (THG1; accession no. AF003347), Arabidopsis EST sequence (At-HisG; accession no. Z31670), *S. cerevisiae* ATP-PRT (Sc-His1; accession no. V01306), *Yarrowia lipoytica* (Yl-His1; accession no. U40563), *Schizosaccharomyces pombe* (Sp-His1; accession no. Z70691), *Hemophilus influenzae* (Hi-HisG; accession no. U32729), *Salmonella typhimurium* (St-HisG; accession no. X13464), *E. coli* ATP-PRT (Ec-HisG; accession no. X13462), *Archaeoglobus fulgidus* (His1-Arcfu; accession no. AE001064), *Methanococcus jannaschii* (His1-Metja; accession no. U67562), and *Methanobacterium thermoautotrophicum* (His1-Metth; accession no. AE000911).

sis of selected samples showed that there were no increases in the amount of His associated with peptides and proteins (data not shown).

X-ray absorption spectroscopy clearly demonstrated that the amount of Ni coordinated by His in both roots and shoots of *T. arvense* always exceeded that found in *T. goesingense* during 1 to 7 d of exposure to 10 μM Ni (Table III). The x-ray absorption edge spectra for Ni-His were significantly different from Ni-imidazole (data not shown); therefore, the x-ray absorption spectroscopy data presented suggest that the Ni-His complex observed in *Thlaspi* tissues represents Ni coordinated with free His and not His residues in proteins.

DISCUSSION

To test the hypothesis that free His plays a role in the mechanism of Ni hyperaccumulation in *T. goesingense*, we investigated the regulation of His biosynthesis at the molecular and biochemical levels, and studied the role of His in Ni coordination in planta. By functionally complementing His auxotrophic *E. coli* mutants with *T. goesingense* cDNAs, we isolated genes (*THG1*, *THB1*, and *THD1*) encoding enzymes that catalyze three steps in the His biosynthetic pathway. The first of these, *THG1*, encodes ATP-PRT, a functional homolog of an enzyme that catalyzes the production of *N*-(5′-phosphoribosyl)-ATP (PR-ATP) from ATP and phosphoribosyl pyrophosphate, the first committed step in His biosynthesis in *E. coli*. This is the first conclusive evidence that ATP-PRT exists in plants and confirms the earlier observation of ATP-PRT-like enzymatic activity in plant tissue extracts (Waiter et al., 1971).

The presence of ATP-PRT in *T. goesingense* also supports the growing body of evidence suggesting that His biosynthesis in plants follows a very similar pathway to that observed in *E. coli* (Nagai et al., 1991; Tada et al., 1993, 1994; Kim and Theologis, 1996; Bevan et al., 1998; El Malki et al., 1998; Fujimori and Ohta, 1998). Because *THG1* is the first example of a gene encoding ATP-PRT in plants, we performed a genomic Southern analysis to determine how many copies of this gene occur in the *T. goesingense* genome. This analysis suggested that there are only a small number of *THG1* genes present in *T. goesingense*, similar to the low copy number of genes encoding HDH and IGPD in *B. oleracea* and Arabidopsis (Nagai et al., 1991; Tada et al., 1994). An investigation of the evolutionary relationships between the *T. goesingense* ATP-PRT and other archaebacteria, eubacteria, and unicellular eukaryotic ATP-PRT sequences placed the plant ATP-PRT on a separate evolutionary branch from the three other groups (Fig. 3). The *T. goesingense* ATP-PRT did cluster with an Arabidopsis EST clone (Z31670) that showed 81% amino acid identity to the *T. goesingense* ATP-PRT amino acid sequence.

Expression of the *T. goesingense THG1* in *E. coli* generated a protein with an apparent molecular mass of 49,000 D, based on SDS-PAGE (data not shown). This corresponds closely to a predicted molecular mass of 49,335 D based on the protein translation product of the fusion of the *THG1*

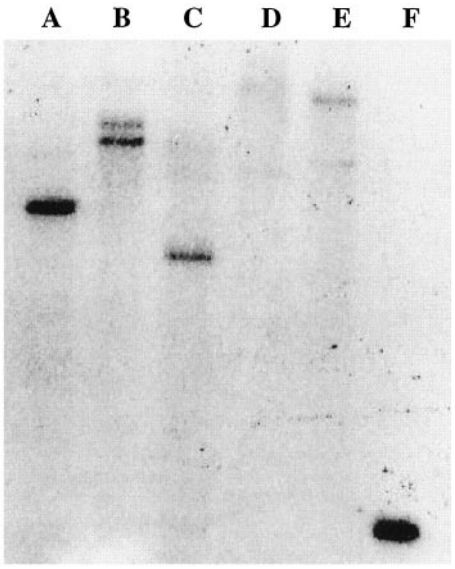

Figure 4. Southern-blot analysis of *T. goesingense THG1*. Genomic DNA was cut with *Bam*HI (lane A), *Eco*RI (lane B), *Hin*dIII (lane C), *Xba*I (lane D), *Xho*I (lane E), and *Pst*I (lane F), and probed with a ^{32}P-labeled *THG1* cDNA fragment.

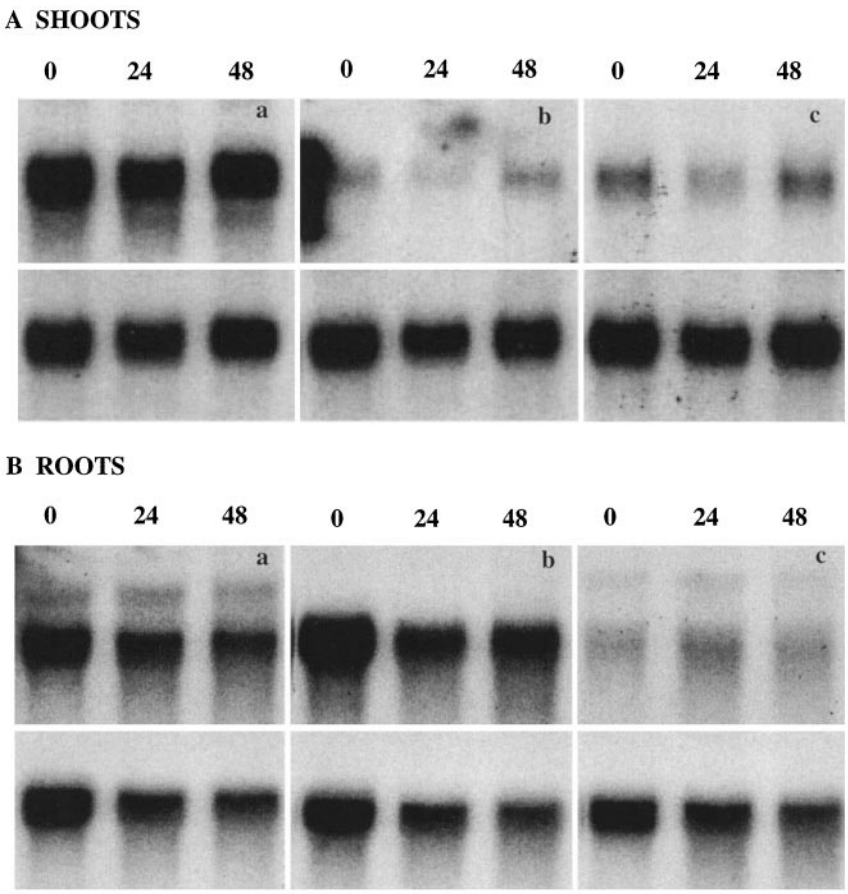

Figure 5. Northern analysis of total RNA isolated from *T. goesingense* exposed to 50 μM Ni for 0, 24, and 48 h showing the expression of *THG1*, *THD1*, and *THB1*. Total RNA was isolated from *T. goesingense* shoot (A) and root (B) tissue and probed with ^{32}P-labeled *THG1* (a), *THB1* (b), and *THD1* (c) cDNAs probes. Bottom rows in both A and B show blots from total RNA being probed with an Arabidopsis ^{32}P-labeled actin cDNA fragment as a loading control.

cDNA sequence and the expression vector sequence. The predicted molecular mass of the *T. goesingense* ATP-PRT after cleavage of the putative chloroplast target sequence, at the predicted cleavage site between amino acids residues 45 and 46, was calculated to be 39,056 D. This is similar to the molecular masses of other ATP-PRTs of approximately 32,500 D (Alifano et al., 1996).

In *E. coli* ATP-PRT is an important control point for His biosynthesis, being regulated at the level of transcription, translation, and allosteric activation/inhibition (Alifano et al., 1996). The highly regulated nature of ATP-PRT in *E. coli* and its role in the catalysis of the first committed step in

Table II. *Free His content of T. goesingense tissues exposed to 50 μM Ni for 7 d*

His was measured by HPLC as the phenylthiocarbamyl amino acid derivative with methionine sulfoxide as the internal standard. n.a., Not available. Data are the means ± SD of between three and eight independent plant samples (nos. in parentheses represent *n*).

	Shoot	Root	Xylem Sap
	nmol g^{-1} fresh biomass		*μmol L^{-1}*
T. goesingense			
Control	136 ± 37 (4)	742 ± 188 (4)	7.4 ± 3 (4)
Nickel-treated	107 ± 62 (5)	68 ± 30 (7)	18.2 ± 9 (6)
T. arvense			
Control	73 ± 16 (4)	43 ± 9 (3)	57 ± 31 (8)
Nickel-treated	n.a.	n.a.	n.a.

Table III. *Nickel coordination by His ligands in T. goesingense and T. arvense measured by x-ray absorption spectroscopy*

Values in parentheses represent the total Ni content of the tissue mmol kg^{-1} dry biomass.

Time (d)	*T. goesingense*		*T. arvense*	
	Shoot	Root	Shoot	Root
	mmol kg^{-1} dry biomass			
1	0.2 (3.0)[a]	2.5 (8.7)	0.4 (0.5)	2.9 (6.2)
3	0.1 (4.2)	2.5 (6.7)	1.0 (2.3)	3.9 (10.6)
5	0.4 (6.5)	2.6 (8.1)	1.2 (2.4)	4.3 (13.0)
7	0.2 (5.3)	4.1 (9.4)	1.3 (3.3)	6.1 (14.8)

[a]Plants were exposed to 10 μM $Ni(NO_3)_2$ in the hydroponic solution. By fitting x-ray absorption spectra of aqueous Ni^{2+} and Ni^{2+} coordinated with His: 6.66 mM $Ni(NO_3)_2$, 80 mM His, 30% (w/v) glycerol, pH 7.0; citrate: 6.66 mM $Ni(NO_3)_2$, 70 mM citrate, 30% glycerol, pH 8.0; Gln: 1 mM $Ni(NO_3)_2$, 4 mM Gln, 30% glycerol, pH 7.3; and isolated *T. goesingense* shoot cell wall material (Lasat et al., 1996), we were able to determine the percentage contribution of His as a ligand of Ni^{2+}. Total Ni content of the tissues was analyzed by inductively coupled plasma emission spectroscopy and this was used to calculate the absolute amount of Ni coordinated by His in the tissues. The values represent data collected from a single plant sample at each time point, and each x-ray spectrum used for the fits represents the mean of three independent scans, each being composed of data acquired from 13 independent detectors.

His biosynthesis suggests that it might also play a key regulatory role in plants, making it a likely target for the regulation of His biosynthesis by Ni. However, northern analysis of the *THG1* RNA message clearly demonstrated that Ni does not induce or suppress transcription of the *THG1* mRNA in either the roots or shoots of *T. goesingense* (Fig. 5). Because it is possible that ATP-PRT is not the key regulated step in His biosynthesis in plants, we also analyzed expression of two other genes in the His biosynthetic pathway, *THB1* and *THD1*, which encode the enzymes IGPD and HDH, respectively. The predicted amino acid sequence of both *THB1* and *THD1* show very high homology to other known plant homologs, suggesting that the His biosynthetic pathway is highly conserved in plants. The IGPD enzyme catalyzes the conversion of imidazolglycerol phosphate to imidazoleacetol phosphate, the first step after the branch point that feeds into the purine recycling pathway. This enzyme also catalyzes the conversion of L-histidinol phosphate to L-histidinol. Because of its key position at a branch point in the His biosynthetic pathway this enzyme may also be regulated. HDH catalyzes the oxidation of L-histidinol to L-hisitidine, the final step in His biosynthesis. Because this catalytic step uses NAD^+ as an oxidant, it is possible that it is also regulated in plants.

Northern analysis of the mRNA levels for both *THB1* and *THD1* clearly showed that expression of these mRNAs is not induced or repressed by Ni treatment in either the roots or the shoots of *T. goesingense* (Fig. 5). Because *THG1*, *THB1*, and *THD1* mRNA expression levels were not changed by Ni treatment, it is unlikely that control of the His biosynthetic pathway at the transcriptional level by Ni is involved in Ni hyperaccumulation in *T. goesingense*.

To determine if Ni modifies His biosynthesis at the post-transcriptional level in *T. goesingense*, we also analyzed the concentration of free His in root, xylem sap, and shoot tissue. It is clear from this data (Table II) that His concentrations remain basically unchanged after Ni exposure in both the xylem sap and the shoots. These biochemical data strongly support the molecular evidence that free His concentrations in *T. goesingense* are not increased by Ni exposure. It is possible, however, that the constitutive concentration of free His observed in *T. goesingense* is sufficient to fulfill its theorized role in Ni hyperaccumulation. To test this hypothesis, we compared the His concentration in *T. goesingense* and the nonaccumulator *T. arvense*. This comparison revealed that the nonaccumulator *T. arvense* contained equal concentrations of His in roots, shoots, and xylem sap as that found in *T. goesingense* during Ni exposure.

The His concentration in the xylem sap of *T. goesingense* after Ni exposure was also similar to that measured in the nonaccumulators *Vitis rotundifolia* and *Lagerstroemia indica* (Anderson and Brodbeck, 1989; Anderson et al., 1993). However, we did observe that roots of *T. goesingense* before Ni exposure had a significantly higher concentration of free His compared with *T. arvense*. An interesting possibility is that His is overproduced in the roots of *T. goesingense* as a Ni-scavenging mechanism to enhance Ni acquisition under low external Ni conditions. Once plants were exposed to a higher Ni concentration, the free His concentration in the roots of the hyperaccumulator were observed to significantly decrease (Table II), and this may reflect the fact that Ni scavenging is no longer required. However, this reduction in His concentration in the roots of the hyperaccumulator was not reflected in reduced expression of *THG1*, *THB1*, or *THD1*. Also, this His loss was not accounted for by increased His concentrations in xylem sap or shoots. It is possible that reduced His concentrations may reflect increased catabolism or efflux of His into roots. However, recent analysis of *T. goesingense* root exudate showed no increases in the rates of His exudation from roots after exposure to Ni (Salt et al., 1999a).

If free His is involved in the hyperaccumulation of Ni, as has been suggested to occur in *Alyssum* species (Krämer et al., 1996), we would predict that His binds Ni within the plant. To directly address this hypothesis we used x-ray absorption spectroscopy to determine the in planta coordination environment of the Ni in both the hyperaccumulator and nonaccumulator *Thlaspi* species (Table III). From these data it was clear that free His or a free-His-like molecule is involved in coordinating Ni in both the roots and shoots of *T. goesingense* and *T. arvense*. However, the concentration of the Ni-His complex in the shoots of the nonaccumulator *T. arvense* appears to be approximately 5- to 10-fold higher than in *T. goesingense*, and equal in the roots, suggesting that increased Ni coordination by His is not a primary determinant of the Ni hyperaccumulation mechanism in *Thlaspi*. Furthermore, the addition of L-His to the culture solution of hydroponically grown *T. arvense* had no effect on the accumulation of Ni in either the root or shoot tissue (data not shown).

Our data suggest that Ni hyperaccumulation in *T. goesingense* is not simply related to an enhanced ability of the hyperaccumulator to accumulate more free His in response to Ni. We would also caution that the role of free His in Ni hyperaccumulation in *Alyssum* remains speculative and will remain so until more detailed mechanistic data are available. For example, using Arabidopsis probes for northern and western analysis in the Ni hyperaccumulator *Alyssum pintodasilvae* (Baker and Brooks, 1989), expression levels of the His biosynthetic enzymes ATP-PRT, IGDH, and HDH were found not to be regulated by Ni (data not shown).

However, there is certain limited evidence suggesting that His may be involved in Ni transport in *Thlaspi* species in general. For example, in this study a significant proportion of root Ni was found to be coordinated by free His ligands in both hyperaccumulator and nonaccumulator *Thlaspi* species. Also, exposure of the nonaccumulator *T. arvense* to D-His was observed to reduce the accumulation of Ni in shoots, but was found to have no effect on root Ni concentrations. This suggests that the D-His-Ni complex may compete with an endogenous L-His-Ni complex for transport to the shoot. However, we would again like to stress that the primary determinant of the Ni hyperaccumulation phenotype in *T. goesingense* is not governed by the overproduction of free His, as has been suggested for *Alyssum* Ni hyperaccumulators.

ACKNOWLEDGMENTS

The authors wish to extend their appreciation to Ingrid Pickering and Roger Prince for their help with x-ray absorption spectroscopy data collection and analysis. The Stanford Synchrotron Radiation Laboratory is funded by the Department of Energy, Office of Basic Energy Sciences, Divisions of Chemical and Materials Science. The Biotechnology Program is supported by the National Institutes of Health, National Center for Research Resources, Biomedical Technology Program. Further support is provided by the Department of Energy, Office of Biological and Environmental Research. We would also like to thank Pamella Motely and Isaac Shaffer for technical assistance, Ilya Raskin for his support of this project, and Richard Meager for providing the Arabidopsis actin cDNA. We would also like to thank the *E. coli* Genetic Stock Center (http://cgsc.biology.yale.edu) for providing the *E. coli* mutant strains.

Received May 28, 1999; accepted August 16, 1999.

LITERATURE CITED

Alifano P, Fani R, Lio Pietro, Lazcano A, Bazzicalupo M, Carlomagno MS, Bruni CB (1996) Histidine biosynthetic pathway and genes: structure, regulation and evolution. Microbiol Rev **60:** 44–69

Andersen PC, Brodbeck BV (1989) Diurnal and temporal changes in the chemical profile of xylem exudate from *Vitis rotundifolia*. Physiol Plant **75:** 63–70

Andersen PC, Brodbeck BV, Mizell RF (1993) Diurnal variations of amino acids and organic acids in xylem fluid from *Lagerstroemia indica*: an endogenous circadian rhythm. Physiol Plant **89:** 783–790

Baker AJM, Brooks RR (1989) Terrestrial higher plants which hyperaccumulate metallic elements a review of their distribution, ecology and phytochemistry. Biorecovery **1:** 81–126

Bevan M, Bancroft I, Bent E, Love K, Goodman H, Dean C, Bergkamp R, Dirkse W, Van Staveren M, Stiekema W (1998) Analysis of 1.9 Mb of contiguous sequence from chromosome 4 of *Arabidopsis thaliana*. Nature **391:** 485–488

Brooks RR, Lee J, Reeves RD, Jaffré T (1977) Detection of nickeliferous rocks by analysis of herbarium specimens of indicator plants. J Geochem Explor **7:** 49–77

Cramer SP, Tench O, Yocum M, George GN (1988) A 13-element Ge detector for fluorescence EXAFS. Nucl Instrum Methods Phys Res **A266:** 586–591

Dawson RMC, Elliott DC, Elliott WH, Jones KM (1986) Data for Biochemical Research, Ed 3. Clarendon Press, Oxford

El Malki F, Frankard V, Jacobs M (1998) Molecular cloning and expression of a cDNA sequence encoding histidinol phosphate aminotransferase from *Nicotiana tabacum*. Plant Mol Biol **37:** 1013–1022

Felsenstein J (1993) PHYLIP (Phylogeny Inference Package) version 3.5c. Distributed by the author. Department of Genetics, University of Washington, Seattle

Fierabracci V, Masiello P, Novvelli M, Bergamini E (1991) Application of amino acid analysis by high-performance liquid chromatography with phenyl isothiocyanate derivatization to the rapid determination of free amino acids in biological samples. J Chromatogr **570:** 285–291

Fujimori K, Ohta D (1998) Isolation and characterization of a histidine biosynthetic gene in Arabidopsis encoding a polypeptide with two separate domains for phosphoribosyl-ATP pyrophosphohydrolase and phosphoribosyl-AMP cyclohydrolase. Plant Physiol **118:** 275–283

George GN (1998) EXAFSPAK, a suite of programs for x-ray absorption spectroscopy data analysis. http://ssrl.slac.stanford.edu/exafspak.html

George GN, Gorbaty ML, Keleman SR, Sansone M (1991) Direct determination and quantification of sulfur forms in coals from the Argonne premium sample program. Energy Fuels **5:** 93–97

Kim J, Theologis A (1996) Cloning a cDNA encoding imidazoleglycerol-phosphate dehydratase, the yeast HIS3 homolog from pea (accession no. U49978) (PGR 96–033). Plant Physiol **111:** 651

Koningsberger DC, Prins R (1988) X-ray Absorption Principles, Applications, Techniques of EXAFS, SEXAFS and XANES. John Wiley, New York

Krämer U, Cotter-Howells JD, Charnock JM, Baker AJM, Smith JAC (1996) Free histidine as a metal chelator in plants that accumulate nickel. Nature **379:** 635–638

Krämer U, Smith RD, Wenzel W, Raskin I, Salt DE (1997) The role of nickel transport and tolerance in nickel hyperaccumulation by *Thlaspi goesingense* Halácsy. Plant Physiol **115:** 1641–1650

Lasat MM, Baker AJM, Kochian LV (1996) Physiological characterization of root Zn^{2+} absorption and translocation to shoots in Zn hyperaccumulator and nonaccumulator species of *Thlaspi*. Plant Physiol **112:** 1715–1722

Murphy A, Taiz L (1995) Comparison of metallothionein gene expression and nonprotein thiols in ten Arabidopsis ecotypes: correlation with copper tolerance. Plant Physiol **109:** 945–954

Myers EW, Miller W (1989) Approximate matching of regular expressions. Bull Math Biol **51:** 5–37

Nagai A, Ward ER, Tada S, Beck JJ, Chang J-Y, Scheidegger A, Ryals JA (1991) Structural and functional conservation of histidinol dehydrogenase between plants and microbes. Proc Natl Acad Sci USA **88:** 4133–4137

Nakai K, Kanehisa M (1992) A knowledge base for predicting protein localization sites in eukaryotic cells. Genomics **14:** 897–911

Nielsen H, Engelbrecht J, Brunak S, Heijne G (1997) Identification of prokaryotic and eukaryotic signal peptides and prediction of their cleavage sites. Protein Eng **10:** 1–6

Persans M, Yan X, Smith R, Salt DE (1998) Cloning of two cDNAs from the Ni hyperaccumulator *Thlaspi goesingense*: histidinol dehydrogenase (accession no. AF023141) and imidazolglycerolphosphate dehydratase (accession no. AF023140), two enzymes in the histidine biosynthetic pathway (PGR98–078). Plant Physiol **117:** 332

Puissant C, Houdebine LM (1990) An improvement of the single-step method of RNA isolation by acid guanidinium thiocyanate-phenol-chloroform extraction. Biotechniques **8:** 148–149

Reeves RD, Brooks RR (1983) European species of *Thlaspi* L. (Cruciferae) as indicators of nickel and zinc. J Geochem Explor **18:** 275–283

Salt DE, Kato N, Krämer U, Smith RD, Raskin I (1999a) The role of root exudates in nickel hyperaccumulation and tolerance in accumulator and non-accumulator species of *Thlaspi*. *In* N Terry, GS Bañuelos, eds, Phytoremediation of Contaminated Soil and Water, Chapter 10. CRC Press, Boca Raton, FL, pp 189–199

Salt DE, Krämer U (1999) Mechanisms of metal hyperaccumulation in plants. *In* BD Ensley, I Raskin, eds, Phytoremediation of Toxic Metals: Using Plants to Clean-Up the Environment, Chapter 13. John Wiley, New York, pp 231–246

Salt DE, Prince RC, Baker AJM, Raskin I, Pickering IJ (1999b) Zinc ligands in the metal hyperaccumulator *Thlaspi caerulescens* as determined using x-ray absorption spectroscopy. Environ Sci Technol **33:** 713–717

Tada S, Volrath S, Guyer D, Scheidegger A, Ryals J, Ohta D, Ward E (1994) Isolation and characterization of cDNAs encoding imidazoleglycerolphosphate dehydratase from *Arabidopsis thaliana*. Plant Physiol **105:** 579–583

Thompson JD, Higgins DG, Gibson TJ (1994) CLUSTAL W: improving the sensitivity of progressive multiple sequence alignment through sequence weighting, position specific gap penalties and weight matrix choice. Nucleic Acids Res **22:** 4673–4680

Waiter A, Krajewska-Grynkiewicz K, Klopotowski T (1971) Histidine biosynthesis and its regulation in higher plants. Acta Biochim Pol **18:** 299–307